Estimation and Control Related Issues in Smart Material Structures and Fluids*

H.T. Banks, Gabriella A. Pinter and Laura K. Potter
Center for Research in Scientific Computation
North Carolina State University
Raleigh, NC 27695-8205 USA

B.C. Muñoz and L.C. Yanyo
Thomas Lord Research Center
Lord Corporation
Cary, NC 27511-7900 USA

Abstract

We discuss issues related to modeling of nonlinearities and hysteresis arising in a class of magnetorheological-based smart elastomers. The dynamic models, intended for use in parameter estimation and control problems, are presented in the context of simple elongation of a filled rubber-like rod. Theoretical, computational and experimental results are given.

1 Introduction

Smart material structures and *fluids* are generally understood to be structure and fluid composites that possess the capability to sense and actuate in a controlled manner in response to variable ambient stimuli. These are in actuality smart material systems which involve combinations of advanced sensors, actuators and microprocessors. Effective practical use of these systems in specific applications depends on fundamental developments related to a number of important modeling issues involving these composites. In particular one must have (i) models for the composite host system including sensors and actuators and (ii) models describing host system responses to input signals to the actuator. The first of these is the inactive host system model while the latter refers to the system undergoing actuation in response to stimulation. For example, detailed discussions of issues related to models for self-sensing, self-actuating structures based on piezoceramic sensors/actuators can be found in [9]. Piezoceramic-based smart systems are a rapidly maturing technological field with a large literature (a substantial number of references are given in [9]). Another class of systems based on magnetorheological (MR) solids and fluids is far less developed and questions related to these systems are the main focus of our discussions in this presentation.

MR elastomers [26],[27], which are solid analogs of MR fluids, are rubber-like composite structures filled with active as well as inactive substances. Magnetically permeable particles (such as carbonyl iron) are added to a viscoelastic polymeric material prior to crosslinking. A strong external magnetic field is applied before and during crosslinking. This field induces dipole moments within the particles, which seek minimum energy states. Particle chains with collinear dipole moments are formed and curing of the polymeric host material locks the chains in place. The resulting product

*Invited Keynote Lecture, 4th International Conference on Optimization: Techniques and Applications, Perth, Australia, July 1-3, 1998.

Report Documentation Page

Form Approved
OMB No. 0704-0188

1. REPORT DATE	2. REPORT TYPE	3. DATES COVERED
JUL 1998		**00-00-1998 to 00-00-1998**

4. TITLE AND SUBTITLE	5a. CONTRACT NUMBER
Estimation and Control Related Issues in Smart Material Structures and Fluids	5b. GRANT NUMBER
	5c. PROGRAM ELEMENT NUMBER
6. AUTHOR(S)	5d. PROJECT NUMBER
	5e. TASK NUMBER
	5f. WORK UNIT NUMBER
7. PERFORMING ORGANIZATION NAME(S) AND ADDRESS(ES) **North Carolina State University,Center for Research in Scientific Computation,Raleigh,NC,27695-8205**	8. PERFORMING ORGANIZATION REPORT NUMBER
9. SPONSORING/MONITORING AGENCY NAME(S) AND ADDRESS(ES)	10. SPONSOR/MONITOR'S ACRONYM(S)
	11. SPONSOR/MONITOR'S REPORT NUMBER(S)

12. DISTRIBUTION/AVAILABILITY STATEMENT
Approved for public release; distribution unlimited

13. SUPPLEMENTARY NOTES

14. ABSTRACT
see report

15. SUBJECT TERMS

16. SECURITY CLASSIFICATION OF:			17. LIMITATION OF ABSTRACT	18. NUMBER OF PAGES	19a. NAME OF RESPONSIBLE PERSON
a. REPORT **unclassified**	b. ABSTRACT **unclassified**	c. THIS PAGE **unclassified**		**17**	

is a composite material with variable elastic modulus (maximum modulus changes of between 30% and 40% have been reported in experimental data [26] in response to an applied external magnetic field).

Models of the response of the elastomer to an applied magnetic field involve induced stress as a function of induced magnetic flux density. This in turn involves understanding the dependence of the elastic modulus on the induced magnetic flux. Modeling, which is truly in its infancy, can be based on magnetic dipole interactions between adjacent particles. Since the value of the magnetic permeability varies dramatically between particles and host material, it is to be expected that homogenization techniques [10], [16], [22] will play a significant role in any careful modeling of effective moduli. Early results [32] suggest that the magnetic permeability is a nonlinear function of the magnetic potential and hence nonlinear homogenization [15] formulations will be necessary to develop models in category (ii) above.

Our discussions here will be on models for the dynamical response of the composite host, i.e., inactive filled elastomers or filled viscoelastic structures. Thus we focus on issues related to requirement (i) above. Such models involve nonlinear and hysteretic formulations in a significant way. We describe some of our efforts with model development, estimation and experimental verification.

2 Nonlinear Constitutive Laws

Our early efforts focused on understanding the nonlinearities inherent in the dynamic response of rubber-like compounds to applied loads and impulsive disturbances. First we outline the development of our basic model, then turn to theoretical foundations and experimental results.

Most models for elastomers found in the literature are based on strain energy function (SEF) and finite strain theories (see [6] and references there). To illustrate our approach (which is based on the same principles), we take a simple example (for a detailed development see [6]): an isotropic, incompressible, rubber-like rod with a tip mass undergoing simple elongation with a finite applied stress in the principle axis direction $x_1 = x$. For neo-Hookean materials the finite stress theory (or the Mooney theory with SEF $U = C_1(I_1 - 3)$) leads to a true stress $T = \frac{E}{3}(\lambda_1^2 - \frac{1}{\lambda_1})$, or an engineering stress

$$S = \frac{T}{\lambda_1} = \frac{E}{3}(\lambda_1 - \frac{1}{\lambda_1^2}).$$

Here λ_i are the principle extension ratios which represent the deformed length of unit vectors parallel to the principal axes (the axes of zero shear stress), and the first strain invariant I_1 is $I_1 = \lambda_1^2 + \lambda_2^2 + \lambda_3^2$. In this case the dynamical problem reduces to a $1 - D$ problem. In terms of the finite strain $\tilde{e}_{xx}$ and the deformation u in the x direction we have

$$\lambda_1^2 = 1 + 2\tilde{e}_{xx} = 1 + 2\frac{\partial u}{\partial x} + \left(\frac{\partial u}{\partial x}\right)^2 = \left(1 + \frac{\partial u}{\partial x}\right)^2.$$

This can be used in the Timoshenko theory for longitudinal vibrations of a rubber bar with a tip mass to obtain (ρ = mass density, $F(t)$ = applied external force, A_c is the cross sectional area, M is the tip mass, g is the gravitational constant)

$$\begin{aligned} \rho A_c \frac{\partial^2 u}{\partial t^2} - \frac{\partial S}{\partial x} &= 0 \qquad 0 < x < \ell \\ M\frac{\partial^2 u}{\partial t^2}(t,\ell) &= -S|_{x=\ell} + F(t) + Mg \end{aligned} \tag{1}$$

where S, the internal stress resultant, is given by

$$S = \frac{A_c E}{3}(\lambda_1 - \frac{1}{\lambda_1^2}) + C_D A_c \frac{\partial \lambda_1}{\partial t} = \frac{A_c E}{3}\tilde{g}\left(\frac{\partial u}{\partial x}\right) + C_D A_c \frac{\partial^2 u}{\partial t \partial x}. \tag{2}$$

Here E is the generalized modulus of elasticity and $\tilde{g}(\xi) = 1+\xi-(1+\xi)^{-2}$. A Kelvin-Voigt damping term is included in the stress as a first attempt to model damping (C_D is the Kelvin-Voigt damping coefficient). This leads to the nonlinear partial differential equation

$$\rho A_c \frac{\partial^2 u}{\partial t^2} - \frac{\partial}{\partial x}\left(\frac{EA_c}{3}\left(\frac{\partial u}{\partial x} + g\left(\frac{\partial u}{\partial x}\right)\right) + A_c C_D \frac{\partial^2 u}{\partial t \partial x}\right) = 0 \qquad 0 < x < \ell \tag{3}$$

$$M\frac{\partial^2 u}{\partial t^2}(t,\ell) = -\left(\frac{EA_c}{3}\left(\frac{\partial u}{\partial x} + g\left(\frac{\partial u}{\partial x}\right)\right) + A_c C_D \frac{\partial^2 u}{\partial t \partial x}\right)|_{x=\ell} + F(t) + Mg \tag{4}$$

$$u(t,0) = 0, \;\; u(0,x) = \Delta(x), \;\; u_t(0,x) = 0, \tag{5}$$

for dynamic longitudinal displacements of a neo-Hookean material rod in extension. Here the initial configuration is given by $\Delta(x)$ and $g(\xi) = \xi - (1+\xi)^{-2}$. This model in variational formulation is given by

$$\rho A_c u_{tt} + \mathcal{A}_1 u + \mathcal{A}_2 u_t + D^* g(Du) = F \quad \text{in} \quad V^*, \tag{6}$$

where V is an appropriately chosen Hilbert space.

Several theoretical and practical questions arise in connection with this model. The most fundamental is the well-posedness of the initial boundary value problem associated with (3)-(5). It is shown in [4] that a unique weak solution of (3)-(5) exists even under more general circumstances, i.e., for a broad class of nonlinearities g. This is important, since comparison between experimental data and preliminary numerical calculations suggested that the neo-Hookean nonlinearity is not adequate to describe the behavior of filled elastomers. To estimate the correct g and the other unknown parameters in (3)-(5), namely, ρ, E, and C_D, free release experiments were performed (for details see [6]).

For the experiments a slender rod composed of unfilled natural rubber was used. The rod had a tip mass to guarantee that it remains in simple extension and compression is not present. Initially, the rod was lifted so that it was at its natural length. Then the support was removed, allowing the mass to fall freely. The rod achieved approximately 34% maximum dynamic strain during this test. The data collected by the load cell on top of the sample were used to estimate the unknown parameters.

In one general parameter estimation formulation, equation (6) takes the form

$$\rho A_c u_{tt} + \mathcal{A}_1(q) u + \mathcal{A}_2(q) u_t + D^* g(q)(Du) = F(q) \tag{7}$$

$$u(0) = \Delta(x), \;\; u_t(0) = 0, \tag{8}$$

where the structural operators $\mathcal{A}_1, \mathcal{A}_2$, the nonlinearity g and the input F have all been parameterized by a vector (possibly infinite dimensional) parameter q that must be estimated. Here the parameter q takes values from an admissible parameter set Q. Suppose that we have a set of measured observations $z = \{z_i\}_{i=1}^K$ corresponding to measurements (e.g., displacements, velocities) taken at time t_i. In a general least squares parameter estimation problem, we seek to minimize the least squares output functional

$$J(q,z) = \left|\tilde{C}_2\left\{\tilde{C}_1\{u(t_i,\cdot;q)\} - \{z_i\}\right\}\right|^2 \tag{9}$$

over $q \in Q$, where $\{u(t_i,\cdot;q)\}$ are the parameter-dependent solutions of (7)-(8) evaluated at time $t_i, i = 1,2,\ldots K$, and $|\cdot|$ is an appropriately chosen Euclidean norm. The operators $\tilde{C}_1, \tilde{C}_2$ depend on the type of the collected data. For example, if z_i is time domain displacement, velocity or acceleration at a point x, then $\tilde{C}_1$ involves differentiation (0,1 or 2 times, respectively) with respect

to time followed by pointwise evaluation in t and x. The operator $\tilde{C}_2$ is the identity in the case of time domain identification, while it is related to the Fourier transform if we consider fitting the data in the frequency domain (see Chapter 5 of [9] for details).

In this formulation the minimization problem involves an infinite dimensional state space and (in general) an infinite dimensional admissible parameter set Q. To overcome this difficulty and to obtain a computationally tractable method, we use the general ideas described in [9]. Namely, let H^N be finite dimensional subspaces of the state space H, and Q^M be a sequence of finite dimensional sets approximating the parameter set Q. Denote the orthogonal projections of H onto H^N by P^N. One can formulate a family of approximating estimation problems with finite dimensional state spaces and finite dimensional parameter sets in the following way: find $q \in Q^M$ which minimizes

$$J^N(q,z) = \left| \tilde{C}_2 \left\{ \tilde{C}_1 \{ u^N(t_i, \cdot; q) \} - \{ z_i \} \right\} \right|^2, \tag{10}$$

where $u^N(t;q) \in H^N$ is the solution to the finite dimensional approximation of (7)-(8) given by:

$$\langle u^N_{tt}, \phi \rangle_{V_2^*, V_2} + \langle \mathcal{A}_1(q) u^N, \phi \rangle_{V^*, V} + \langle \mathcal{A}_2 u^N_t, \phi \rangle_{V_2^*, V_2} + \langle g(q)(Du^N), D\phi \rangle$$
$$= \langle F(t;q), \phi \rangle_{V_2^*, V_2} \tag{11}$$

$$u^N(0) = P^N \Delta(x), \; u^N_t(0) = 0 \tag{12}$$

for all $\phi \in H^N$. Here $V \hookrightarrow V_2 \hookrightarrow H$ in a Gelfand quintuple (see [9]).

Solution of these approximate estimation problems (10)-(12) provides one with a sequence of parameter estimates $\{\bar{q}^{N,M}\}$. A crucial question is if one can guarantee that this sequence (or some subsequence) converges to a solution of the original infinite dimensional parameter estimation problem. Under certain suitable assumptions on the approximating spaces H^N and approximating sets Q^M, it is shown in [11] that $\bar{q}^{N,M} \to q^*$, where q^* solves the parameter estimation problem for (9).

The above scheme was implemented using linear splines to generate the approximating state spaces and to approximate the nonlinear term g (see [6]). Figure 1 depicts the best fit to the data that can be achieved using a linear g, and definitely suggests that a nonlinear function is required to successfully model the behavior of the rubber rod. Figure 2 depicts the fit achieved using a four-term piecewise linear g. This fit is much better and captures the nonlinear behavior as well. However, as the same experiments and calculations were repeated for medium and highly filled elastomer rods, the best attainable fit deteriorated, indicating that in these cases the hysteretic behavior also must be taken into account.

3 Hysteretic Models

3.1 Conceptual Issues

The efforts described above on nonlinear aspects of rubber dynamics also conclusively demonstrated the (not surprising) importance of hysteresis in our understanding of filled host dynamic response. This is an often studied and seldom resolved aspect of viscoelastic material dynamics which usually begins with constitutive stress-strain formulations. A huge literature on modeling of viscoelastics and rubbers currently exists (e.g., [12], [14], [19], [34], among the many discussed in [35]). Two types of models for stress-strain relationships can be found in the literature on viscoelastic materials. One is developed on the basis of the phenomenological mechanical behavior of the samples, while the other concentrates on the microscopic behavior of the fibers, such as the changes in the crosslinking and the contour length of fibers, and on the different relaxation times of fibers. The most fundamental model is the Boltzmann integral model, which attempts to capture the viscosity

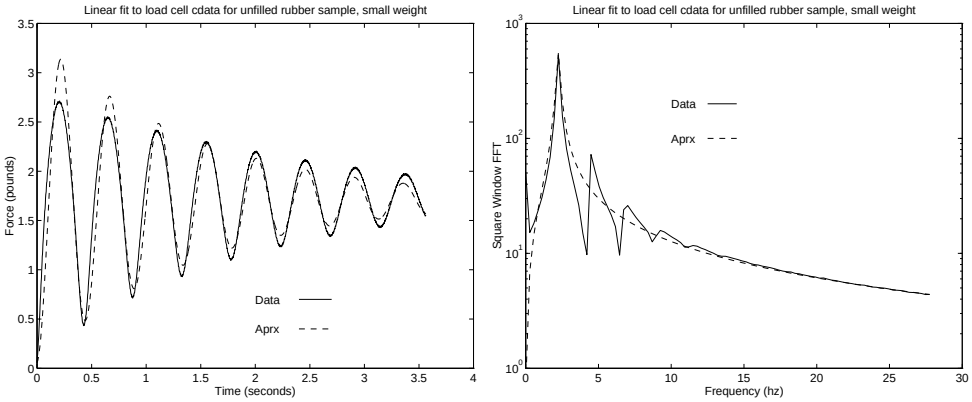

Figure 1: (left) Time domain approximation with a linear g, and (right) the FFT of the solution and the data.

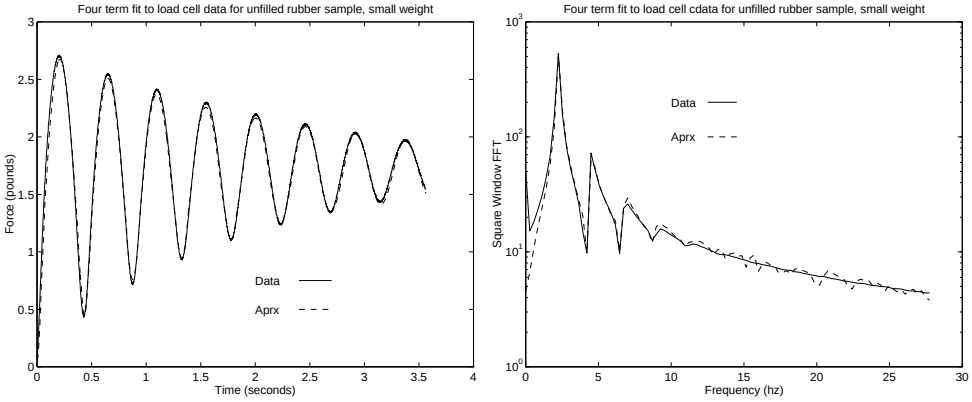

Figure 2: (left) Time domain approximation with a four-term piecewise linear g, and (right) the FFT of the solution and the data.

of the material and the history dependence of the stress on the strain and/or strain rate; the latter characteristic is a signature of rubber materials. As is well known, the Boltzmann integral can be reduced easily to some well-known differential models, e.g., Kelvin-Voigt and Maxwell. Due to the fundamental importance of the Boltzmann integral, we digress here to briefly outline its foundation.

The major assumption (a principle of superposition) made by Boltzmann is that linear models can be added together to generate more complicated models (see [28]). This assumption is referred to as the Boltzmann Superposition Principle (see [18], p. 6).

One can generalize the basic Kelvin-Voigt and Maxwell models (see [35], Chap. 3 for a detailed discussion) to relate the stress and strain by

$$\varepsilon(t) = \sigma_0 J(t)[H(t)] \quad \text{where} \quad \sigma = \sigma_0[H(t)] \tag{13}$$

$$\sigma(t) = \varepsilon_0 Y(t)[H(t)] \quad \text{where} \quad \varepsilon = \varepsilon_0[H(t)] \tag{14}$$

for functions $J(t)$ and $Y(t)$ that are termed the creep compliance function and the relaxation modulus function, respectively. Here H is the usual Heaviside function. Boltzmann generalized the above models to account for variables $\sigma(t)$ and $\varepsilon(t)$ (e.g., the results from stretch and relaxation tests) by considering a succession of infinitesimal steps $d\varepsilon(t)$ for (13) or a succession of infinitesimal steps $d\sigma(t)$ for (14).

As a result, one obtains

$$d\sigma(t) = d\varepsilon(s)Y(t-s)[H(t-s)] \ . \tag{15}$$

One can rewrite $d\varepsilon(s) = \frac{d\varepsilon(s)}{ds}ds$, set $t \geq s$, and integrate (15) from $-\infty$ to t to obtain

$$\sigma(t) = \int_{-\infty}^{t} Y(t-s)\frac{d\varepsilon(s)}{ds}ds \ .$$

A similar expression for ε in terms of the kernel J and the history of the stress rate can be obtained. The above integral is referred to as a Boltzmann integral since it conforms with the fundamentals of superposition as enunciated by Boltzmann. Physical models that consist of a continuum of springs and dashpots are often associated with such integrals since they result from the limit of summing an infinite number of Maxwell and Kelvin-Voigt models (see [18], [35]).

Typical nonlinear behaviors of the stress and strain in rubber materials under finite (i.e., non-infinitesimal) deformation include a continuous increase of strain at decreasing rates upon loading, variable magnitudes of the strain subject to rates of loading, and different loading and unloading paths due to hysteretic memory effects. In addition, there are other nonlinear features that are particular to the samples under study. These traits can be modeled accurately to some degree using theories for finite deformations alone; however, to fully describe nonlinear viscoelastic materials, it is desirable to also consider internal chemical and physical interactions involving long chain molecules and fillers. We refer the reader to [23] for the derivations of internal variable models and internal solid models, which are based on the molecular point of view. The previously mentioned Kelvin-Voigt model, Maxwell model and Boltzmann integral formulation can be modified to include finite deformations by making material coefficients functions of $\varepsilon(t)$ and t, or by defining new laws between $\sigma(t)$ and $\varepsilon(t)$. There are a number of models that involve attempts to model nonlinearity in viscoelastic material through finite deformation theories (see [18], [23], [33]). For more complete discussions we refer readers to Chapter 3 of [35] and a lengthy list of references found there.

Many of the various models in the literature have been verified qualitatively and/or numerically for certain samples under individual tests. However, due to the complex dependence of rubber materials on many physical parameters, it has been very difficult to obtain a general formulation that is reasonably simple quantitatively and that captures viscoelastic behavior across a wide range of materials. For our investigations reported on here, we have used a Boltzmann law with a nonlinear strain functional. Before turning to a summary of our findings to date, we briefly discuss the often controversial subject of pseudo-phenomenological models versus physics-based or internal models in viscoelasticity.

As we have already noted, among the most often used formulations to account for hysteresis is the Boltzmann superposition model (also called the Maxwell solid in history integral form) which is based on the hypothesis that the stress is strain rate dependent through a convolution relationship [14]

$$\sigma(t) = C\varepsilon(t) + \int_{-\infty}^{t} k(t-\tau)\dot{\varepsilon}(\tau)\, d\tau\,. \tag{16}$$

For many materials, this linear relationship is inadequate to capture the behavior and internal characteristics manifested in experiments and one must turn to nonlinear generalizations of the form

$$\sigma(t) = f_e(\varepsilon(t)) + \int_{-\infty}^{t} k(t-\tau) f_v(\dot{\varepsilon}(\tau))\, d\tau \tag{17}$$

or

$$\sigma(t) = f_e(\varepsilon(t)) + \int_{-\infty}^{t} k(t-\tau)\frac{d}{d\tau} f_v(\varepsilon(\tau))\, d\tau\,. \tag{18}$$

The nonlinearities f_e and f_v are often associated with the material's elastic and viscoelastic properties, respectively. Even if one or both are assumed linear, they must be identified along with the kernel k from experimental data. If this is done with little or no mechanistic assumptions that place constraints on the form of f_e, f_v, k (e.g., see [1],[2],[3] and references therein), such an approach renders the Boltzmann modeling a phenomenological approach. If, on the other hand, one uses physical considerations (such as in [8]) to constrain the choices of f_e, f_v, k in the inverse problem or parameter estimation procedures, the modeling attempt can be thought of as pseudo-phenomenological. In fact, it is equivalent to identifying the impulse response function for certain types of (possibly physically-based) internal variable models (Maxwell solids in differential form). For example, if one considers internal strain models as in [24], then the basic assumption is that one has a finite number of internal "strain" variables $\varepsilon_j(t)$, $j = 1, \cdots, N$, along with the strain $\varepsilon(t)$, and the stress is given by

$$\sigma(t) = f_e(\varepsilon(t)) + \sum_{j=1}^{N} c_j \varepsilon_j(t)\,. \tag{19}$$

The internal strains might be given by dynamics

$$\frac{d\varepsilon_j}{dt} + \frac{\varepsilon_j}{\tau_j} = f_j(\dot{\varepsilon}(t))\ ,\ j = 1, \cdots, N\,, \tag{20}$$

or

$$\frac{d\varepsilon_j}{dt} + \frac{\varepsilon_j}{\tau_j} = \frac{d}{dt} f_j(\varepsilon(t)) = f_j'(\varepsilon(t))\dot{\varepsilon}(t)\ ,\ j = 1, \cdots, N\,. \tag{21}$$

If we write the solutions of the equations by

$$\varepsilon_j(t) = \int_{-\infty}^{t} e^{-(t-\tau)/\tau_j} f_j(\dot{\varepsilon}(\tau))\, d\tau \tag{22}$$

or

$$\varepsilon_j(t) = \int_{-\infty}^{t} e^{-(t-\tau)/\tau_j} \frac{d}{d\tau} f_j(\varepsilon(\tau))\, d\tau\,, \tag{23}$$

then (19) is completely equivalent to (17) or (18) where

$$k(t-\tau) f_v(\dot{\varepsilon}(\tau)) = \sum_{j=1}^{N} c_j e^{-(t-\tau)/\tau_j} f_j(\dot{\varepsilon}(\tau)) \tag{24}$$

or

$$k(t-\tau)\frac{d}{d\tau}f_v(\varepsilon(\tau)) = \sum_{j=1}^{N} c_j e^{-(t-\tau)/\tau_j}\frac{d}{d\tau}f_j(\varepsilon(\tau))\,, \tag{25}$$

respectively. In this case, the Boltzmann approach under the assumptions (24) or (25) is completely equivalent to the internal variable approach. The only real difference in these two approaches lies in the implementation; i.e., one might start with (17) or (18) and attempt to identify the overall impulse response function $k(t)$ without any consideration of internal dynamics, or one might use (19) with (20) or (21) and attempt to identify the individual decay constants τ_j along with the coefficients c_j and f_j.

If, however, one assumes nonlinear internal dynamics of the form

$$\frac{d\varepsilon_j}{dt} + g_j(\varepsilon_j) = f_j(\dot{\varepsilon_j})\ ,\ j = 1, \cdots, N, \tag{26}$$

in place of (20), then (19) cannot be rewritten in Boltzmann form and the internal variable approach is distinct from a general Boltzmann approach. In this case, one must solve a coupled system (the overall dynamical PDE in which σ appears plus the system (26) coupled with (19)) as opposed to an implicit internal dynamics system involving (17) or (18) in the PDE's of deformation.

One might also generalize the internal variable/Boltzmann linear models by defining a generalized stress $\overline{\sigma} = (\sigma, \dot{\sigma}, \cdots, \sigma^{(n_1)})$ and generalized strain $\overline{\varepsilon} = (\varepsilon, \dot{\varepsilon}, \cdots, \varepsilon^{(n_2)})$ with internal vector dynamics

$$\frac{d\overline{\sigma}}{dt} = A\overline{\sigma} + \overline{\mathcal{F}}(\overline{\varepsilon}) \tag{27}$$

so that

$$\overline{\sigma}(t) = \int_{-\infty}^{t} e^{A(t-\tau)}\overline{\mathcal{F}}(\overline{\varepsilon}(\tau))\,d\tau\,.$$

If we define $X(t) = e^{At}$, this becomes

$$\sigma(t) = \int_{-\infty}^{t}\sum_{j=1}^{n_1} X_{1j}(t-\tau)\overline{\mathcal{F}}_j(\varepsilon(\tau), \dot{\varepsilon}(\tau), \cdots, \varepsilon^{(n_2)}(\tau))\,d\tau, \tag{28}$$

which again is recognized as a generalized Boltzmann formulation. In particular, (18) is a special case of this formulation with $n_1 = 1$ since

$$\frac{d}{d\tau}f_v(\varepsilon(\tau)) = f_v'(\varepsilon(\tau))\dot{\varepsilon}(\tau) = \mathcal{F}(\varepsilon(\tau), \dot{\varepsilon}(\tau))\,. \tag{29}$$

The internal strain models of (19) and (20) can also be put in this more general form by taking $\tilde{\varepsilon} = (\varepsilon_1, \varepsilon_2, \cdots, \varepsilon_N)$ and

$$\frac{d\tilde{\varepsilon}}{dt} = A\tilde{\varepsilon} + \mathcal{F}(\dot{\varepsilon}(t))$$

so that

$$\tilde{\varepsilon}(t) = \int_{-\infty}^{t} e^{A(t-\tau)}\mathcal{F}(\dot{\varepsilon}(\tau))\,d\tau$$

and

$$\sigma(t) = f_e(\varepsilon(t)) + \overline{c}\cdot\tilde{\varepsilon}(t) = f_e(\varepsilon(t)) + \int_{-\infty}^{t}\overline{c}\cdot\left[e^{A(t-\tau)}\mathcal{F}(\dot{\varepsilon}(\tau))\right]\,d\tau \tag{30}$$

for $\overline{c} = (c_1, c_2, \cdots, c_N)$. These considerations clearly reveal that (19) and (20) are special cases of a generalized Boltzmann approach, and the primary difference between a Boltzmann and linear

internal variables approach is mainly philosophical. That is, in the Boltzmann approach, one attempts to identify the impulse response e^{At} as opposed to the internal variables approach where one is concerned with the operator A. In both situations, one must also identify the nonlinearities f_e and f_v (or $\mathcal{F}$ in (30)).

There is another pseudo-phenomenological approach to hysteresis found in the engineering literature on viscoelasticity that is related to our remarks above. The so-called Golla-Hughes-McTavish (or GHM) method (see [20], [21], [29] for readable summaries) can be interpreted as a nonphysics-based internal variable model approach to viscoelasticity. In this approach, one introduces additional coordinates (i.e., internal variables) in state space models to account for hysteretic behavior. The general approach uses complex modulus or loss factor data (modulus or frequency data) to fit rational polynomials representing the Laplace transform of hysteresis stress-strain relationships. Specifically, the viscoelastic hysteresis is approximated by adjoining a state variable z with frequency domain representation

$$h(s) = \frac{\alpha s^2 + \beta s}{s^2 + bs + c}\,.$$

This is equivalent to an internal dynamics of the form $\ddot{\sigma}_{ve} + b\dot{\sigma}_{ve} + c\sigma_{ve} = \alpha\ddot{\varepsilon} + \beta\dot{\varepsilon}$, or, in frequency domain, $\hat{\sigma}_{ve}\{s^2 + bs + c\} = \{\alpha s^2 + \beta s\}\hat{\varepsilon}$. This, of course, can be recognized as a special case of (27) by defining $\overline{\sigma} = (\sigma_{ve}, \dot{\sigma}_{ve})$, $\overline{\varepsilon} = (\varepsilon, \dot{\varepsilon}, \ddot{\varepsilon})$ and

$$\dot{\overline{\sigma}} = K\overline{\sigma} + E\overline{\varepsilon} \tag{31}$$

with

$$K = \begin{pmatrix} 0 & 1 \\ c & b \end{pmatrix} \quad , \quad E = \begin{pmatrix} 0 & 0 & 0 \\ 0 & \beta & \alpha \end{pmatrix}\,.$$

In the usual engineering practice, one attempts to identify c, b, α, β using frequency domain data and then adjoins this to the time domain (e.g., finite element or modal) model via (31). Once again, the philosophy of this approach is to identify the operator A (i.e., K) in (27) instead of identifying e^{At}.

The internal variable approach outlined above can be carried out for particular structures and materials by hypothesizing physics-based internal dynamics. One such example involves finite strain internal stretch variable models for viscoelastic rubbers as developed by [17] and [25]. These involve stick-slip models for the viscoelastic response to a large step-strain (see [17] and [25] for details).

3.2 Theoretical Issues

To outline our efforts to date in incorporating hysteresis in our models, we return to the example involving simple extension in a rod of cross-sectional area A_c, length ℓ, mass density ρ with applied force $f(t)$ at the end $x = \ell$. We assume a stress-strain law of the form

$$\sigma(t) = g_e(\varepsilon(t)) + \int_{-\infty}^{t} Y(t-s)\frac{d}{ds}g_v(\varepsilon(s), \dot{\varepsilon}(s))ds, \tag{32}$$

where g_e and g_v are nonlinear functions accounting for the elastic and viscoelastic nonlinear response of the rubber rod. Our experimental quasi-static data curves (see below) indicate that the rubber follows different nonlinear viscoelastic constitutive relationships in loading ($\dot{\varepsilon} > 0$) and unloading ($\dot{\varepsilon} < 0$), i.e.,

$$g_v(\varepsilon(s), \dot{\varepsilon}(s)) \;\; = \;\; \begin{cases} g_{vi}(\varepsilon(s)) & \dot{\varepsilon}(s) > 0 \\ g_{vd}(\varepsilon(s)) & \dot{\varepsilon}(s) < 0, \end{cases} \tag{33}$$

where g_{vi} and g_{vd} are continuous nonlinear functions. Note that $g_{vi}(\varepsilon(t_i))$ is not necessarily equal to $g_{vd}(\varepsilon(t_i))$ at the "breakpoints" t_i, i.e., the points where $\dot{\varepsilon}$ changes sign. Thus, we must interpret the derivative in (32) in a distributional sense. Earlier calculations and experiments suggest that the rubber does not exhibit infinite memory, but significantly depends only on history of finite length r. That is, the memory kernel Y is such that $Y(\xi) \approx 0$ for $\xi \geq r$. Therefore we can approximate (32) by

$$\sigma(t) = g_e(\varepsilon(t)) + \int_{t-r}^{t} Y(t-s)\frac{d}{ds}g_v(\varepsilon(s), \dot{\varepsilon}(s))ds. \tag{34}$$

Let us suppose that the t_i are indexed so that the rubber is unloading for $t_k < t < t_{k+1}$, k odd. Integrating by parts in (34) and assuming $t_K < t < t_{K+1}$, where K is odd, we have

$$\begin{aligned}
\sigma(t) &= g_e(\varepsilon(t)) + \int_{t-r}^{t} \dot{Y}(t-s)\frac{d}{ds}g_v(\varepsilon(s), \dot{\varepsilon}(s))ds - Y(r)g_{vi}(\varepsilon(t-r)) + Y(0)g_{vd}(\varepsilon(t)) \\
&+ \sum_{k=1}^{K} Y(t-t_k)(-1)^{k+1}[g_{vi}(\varepsilon(t_k)) - g_{vd}(\varepsilon(t_k))] \\
&= g_e(\varepsilon(t)) + \int_{t-r}^{t} \dot{Y}(t-s)\frac{d}{ds}g_v(\varepsilon(s), \dot{\varepsilon}(s))ds + Y(0)g_{vd}(\varepsilon(t)) \\
&+ \sum_{k=1}^{K} Y(t-t_k)(-1)^{k+1}[g_{vi}(\varepsilon(t_k)) - g_{vd}(\varepsilon(t_k))],
\end{aligned}$$

where we have used $Y(r) \approx 0$. A similar expression holds for loading, i.e., $t_K < t < t_{K+1}$, K even. This is the form of the stress-strain law that we used in the calculations reported on below.

To develop the corresponding dynamic model, we must incorporate these jump terms into our formulation. Let $u(t,x)$ denote the displacement at time t of the section of the rod originally located at x, $0 \leq x \leq \ell$. If we assume that the rod begins its motion at rest with possible deformation $\Delta(x)$ and fixed end at $x = 0$, we obtain the model for unloading, i.e., $t_K < t < t_{K+1}$, K odd,

$$\begin{aligned}
\rho A_c \frac{\partial^2 u}{\partial t^2} &= \frac{\partial}{\partial x}\left(A_c g_e(\frac{\partial u}{\partial x}) + A_c Y(0) g_{vd}(\frac{\partial u}{\partial x}) + A_c \int_{t-r}^{t} \dot{Y}(t-s) g_v(\frac{\partial u}{\partial x}(s), \frac{\partial^2 u}{\partial t \partial x}(s))ds \right. \\
&+ \left. A_c \sum_{k=1}^{K} Y(t-t_k)(-1)^{k+1}[g_{vi}(\frac{\partial u}{\partial x}(t_k)) - g_{vd}(\frac{\partial u}{\partial x}(t_k))] \right) \quad 0 < x < \ell
\end{aligned} \tag{35}$$

$$\begin{aligned}
&\left(A_c g_e(\frac{\partial u}{\partial x}) + A_c Y(0) g_{vd}(\frac{\partial u}{\partial x}) + A_c \int_{t-r}^{t} \dot{Y}(t-s) g_v(\frac{\partial u}{\partial x}(s), \frac{\partial^2 u}{\partial t \partial x}(s))ds \right. \\
&\left. + A_c \sum_{k=1}^{K} Y(t-t_k)(-1)^{k+1}[g_{vi}(\frac{\partial u}{\partial x}(t_k)) - g_{vd}(\frac{\partial u}{\partial x}(t_k))]) \right) |_{x=\ell} = f(t).
\end{aligned} \tag{36}$$

In general this model should be written in variational form

$$\begin{aligned}
&\rho A_c \ddot{u} - \frac{\partial}{\partial x}\left(A_c g_e(\frac{\partial u}{\partial x}) + A_c Y(0) g_{vd}(\frac{\partial u}{\partial x}) + A_c \int_{t-r}^{t} \dot{Y}(t-s) g_v(\frac{\partial u}{\partial x}(s), \frac{\partial^2 u}{\partial t \partial x}(s))ds \right. \\
&\left. + A_c \sum_{k=1}^{K} Y(t-t_k)(-1)^{k+1}[g_{vi}(\frac{\partial u}{\partial x}(t_k)) - g_{vd}(\frac{\partial u}{\partial x}(t_k))] \right) = F(t) \quad \text{in } V^*
\end{aligned} \tag{37}$$

for an appropriately chosen Hilbert space V. This presumes, of course, that we have sufficient smoothness so that evaluation of $\frac{\partial u}{\partial x}$ at t_i makes sense and $\frac{\partial}{\partial x}(g_{vi}(\frac{\partial u}{\partial x}(t_i))) \in V^*$. Note that the jump terms and the related theoretical issues do not appear if we suppose that $g_{vi} = g_{vd} = g_v$. In this case we can take $V = H_L^1(0,\ell)$, $H = L^2(0,\ell)$. If we separate and consider only the linear part, i.e., if $g_e(\xi) = E\xi + h_e(\xi)$ and $g_v(\xi) = E\xi + h_v(\xi)$, and we ignore h_e, h_v, we obtain

$$\rho A_c \ddot{u} - \frac{\partial}{\partial x}(EA_c(1+Y(0))\frac{\partial u}{\partial x} + EA_c\int_{t-r}^{t} \dot{Y}(t-s)\frac{\partial u}{\partial x}(s)ds) = F(t)\ . \tag{38}$$

Following an approach we have used in earlier treatments of Boltzmann or time hysteresis stress-strain laws ([1], [2], [7], [8]), we may write our model as an abstract system in a Hilbert space and develop a semigroup formulation for (38) (see [7],[8]). This in turn can be used to define (implicitly) mild solutions for the nonlinear system in terms of a nonlinear variation-of-parameters representation.

For the linear part of the system, one can also develop a variational formulation to obtain an equivalent well-posedness framework. Our current efforts are devoted to developing the variational formulation and corresponding existence, uniqueness, etc., for the full nonlinear system with jump terms.

3.3 Experimental Quasi-static Results

In a series of experiments at Lord Corporation, we tested filled rubber rods in simple uniaxial tensile deformations. Both ends of the rods were manufactured with metal flanges to be secured in a test machine, the Instron machine, which has a movable load cell that can apply tension to one end of the rod while keeping the other end fixed. The software package STD4200 was used to drive the Instron machine and to produce load-displacement curves upon loading and unloading the samples. Denoting the loading force by $f(t)$, the displacement by $\Delta\ell(t)$, the original length of the rod by ℓ, and the original area of the rod by A_c, we calculate the engineering stress $\sigma(t) = \frac{f(t)}{A_c}$ and the strain $\varepsilon(t) = \frac{\Delta\ell(t)}{\ell} \times 100\%$. Two types of sample rods were used: ones filled with carbon black (CB) and ones filled with silicon (Sil). Quasi-static ($\ddot{u} = 0, \dot{u} = 5$ in/min) stretching/relaxation tensile cycles were performed on samples.

For each percent strain, the sample undergoes three cycles of loading and unloading to remove possible small scale Mullin's effects; this results in stress softening (see [8]). We found that the first cycle had higher values for the loads than the second and third loops. (Mullin's effect is very significant at the initial pulls on the sample. In fact, the CB filled sample was first pulled to approximately 300% strain and the Sil filled sample was pulled to 150% strain before we recorded data for lower percent strains.) We used the third cycle for each percent strain for our parameter estimation problems in the results presented here.

We report here on results for a CB rod ($\ell = 6.13$ in, diameter $= .54$ in after removal of Mullin's effects) and a Sil rod ($\ell = 7.455$ in, diam $= .505$ in). We assumed no initial strain history for the rubber samples, and we used the following stress-strain relationship for our computations:

$$\sigma(t) = g_e(\varepsilon(t)) + \int_{t-r}^{t} Y(t-s)\frac{dg_v(\varepsilon(s),\dot{\varepsilon}(s))}{ds}ds, \tag{39}$$

where Y is the memory kernel, and g_e and g_v represent the elastic response and viscoelastic response respectively. As before, r is defined so that $Y(r) \approx 0$.

This model conveniently provides a starting point for modeling the hysteresis curves. The challenge is to identify plausible memory kernels and response functions g_e, g_v.

Based on previous experimental studies (see [35]), we chose an exponential form for the memory kernel Y. Such an exponential form generates totally nested hysteresis loops in the stress-strain

curves, a feature we also observed in our experimental data. For C_2 and C_3 positive, we define

$$Y(t) = C_2 e^{-C_3 t}. \tag{40}$$

The inclusion of both elastic and viscoelastic response functions resulted from both experimental observations and earlier work (e.g., see [23], [25]). Elastic materials undergoing finite deformations require the use of a nonlinear constitutive law, which suggests that rubber materials would also have a nonlinear function in the stress-strain relationship. Moreover, filled rubber exhibits viscoelastic and hysteretic properties, which leads to the use of the viscoelastic response function inside the integral.

We tried a number of linear and nonlinear viscoelastic response functions (see [35] for details). The relative errors discussed in [35] suggested that a nonlinear function $g_v(\varepsilon(t))$ is necessary for both the CB data and the Sil data taken at sufficiently large strains. Looking closely at the data, it seemed that the viscoelastic response of the rubber during loading was significantly different than the response while unloading. As a result, we include separate functions g_{vi} and g_{vd} in the viscoelastic response g_v, where g_{vi} represents the response while $\varepsilon(t)$ is increasing, and g_{vd} represents the response when $\varepsilon(t)$ is decreasing. This means that g_v is now a function of both ε and $\dot{\varepsilon}$, with the form given in (33).

Additional curve fitting studies outlined in [35] led to our choice of cubic polynomials for the viscoelastic response. That is, $g_{vi}(\varepsilon) = \sum_{k=0}^{3} a_k \varepsilon^k$ and $g_{vd}(\varepsilon) = \sum_{k=0}^{3} b_k \varepsilon^k$, where $\{a_k, b_k\}$ are parameters to be determined by estimation techniques.

The form for the elastic response g_e was chosen in a similar manner. Preliminary results suggested that a cubic polynomial was also a good choice for the elastic response. We define g_e by $g_e(\varepsilon) = \sum_{k=0}^{3} E_k \varepsilon^k$, where E_k are parameters to be determined.

The parameters $\{C_k, E_k, a_k, b_k\}$ were estimated by fitting stress-strain data, i.e. minimizing

$$\sum_{k=1}^{N} |\sigma(t_k) - \hat{\sigma}(t_k)|^2 \tag{41}$$

for stress data $\hat{\sigma}$. The single-loop data sets used for estimation include a Sil sample stretched to 100% strain, and a CB sample stretched to 200% strain. These strain levels were chosen because the data exhibited both strong nonlinear and hysteretic characteristics. The results are presented in Figures 3 and 4. The relative errors are at satisfactory levels, and the shapes of the loops are closely matched.

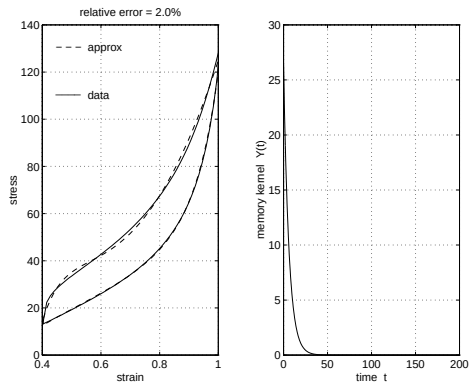

Figure 3: Sil rod, 100% strain: (left) stress-strain with cubic g_e, cubic g_v; (right) corresponding exponential kernel.

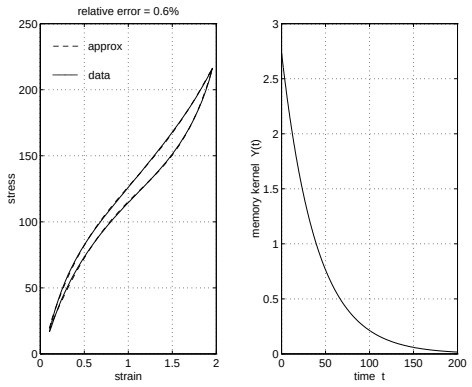

Figure 4: CB rod, 200% strain: (left) stress-strain with cubic g_e, cubic g_v; (right) corresponding exponential kernel.

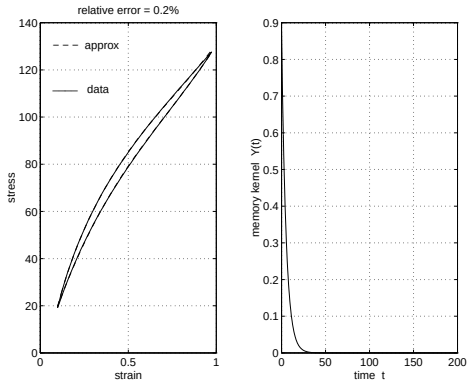

Figure 5: CB rod, 100% strain: (left) stress-strain with cubic g_e, cubic g_v; (right) corresponding exponential kernel.

After estimating the parameters with the above data sets, we used these parameters to predict the stress for smaller strain loops of the same rubber sample. These predictions were quite accurate for strain levels within 40 percent of the strain level used for the original fitting (i.e., strains at 180% and 160% for the 200% strain data fit, and strains at 80% and 60% for the 100% strain data fit), but the accuracy declined greatly as the strain level decreased. These observations and similar findings by [24] suggest that one parameter set may not sufficiently capture the stress-strain relationship for filled rubber. Looking closely at the CB data, it appears that both the nonlinearity and the hysteresis were quite different at small strain levels versus large strain levels. Indeed, these observations led to the conclusion that both a large strain model and a small strain model are needed.

Since the parameters obtained from the CB 200% data set predicted loops more accurately at larger strains than smaller strains, we chose this parameter set as our large strain model for the CB sample. We then performed a separate fitting to the CB 100% data to obtain a small strain model. These results were similarly satisfactory in terms of both the relative error and the shape of the loop (see Figure 5), and these parameters produced accurate predictions of the stress for 80% and 60% strain loops.

In addition to the accurate prediction of smaller individual strain loops, another desirable feature

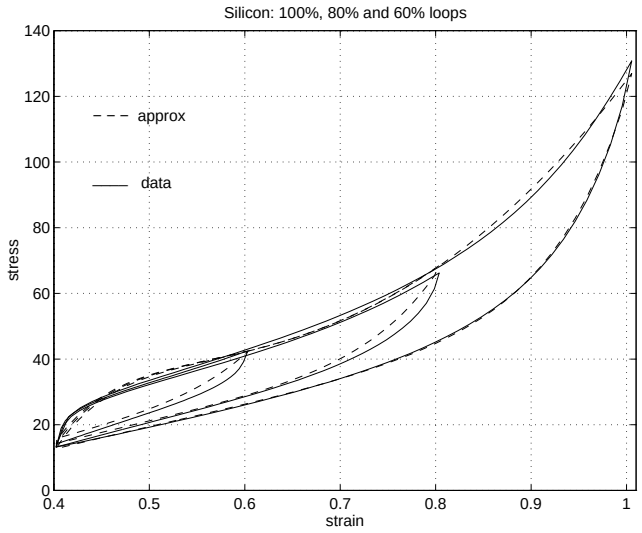

Figure 6: Sil rod, response to 100%, 80%, 60% strains: 100% strain parameter set, predicted nested loops for 80%, 60% strains; relative error = 3.6%.

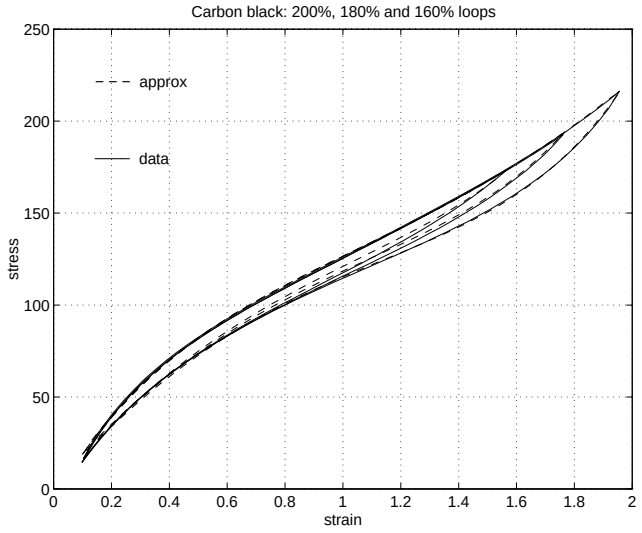

Figure 7: CB rod, response to 200%, 180%, 160% strains: 200% strain parameter set, predicted nested loops for 180%, 160% strains; relative error = 1.2%.

of the stress-strain relation is the ability to predict nested loops consecutively in time. When the parameters are used to predict individual strain loops, no previous history is assumed and the calculations are made with one strain loop only. Predicting nested loops, however, requires the inclusion of all previous strain loops as a part of the history.

After obtaining the fittings for Sil 100%, CB 200% and CB 100%, the parameter sets were used to predict the inner loops. For the 100% fittings, the inner loops correspond to 80% and 60% strain levels, and for the 200% fitting, the inner loops are at 180% and 160% levels. Results are presented in Figures 6, 7 and 8. The predictions are quite satisfactory with respect to both relative error and shape.

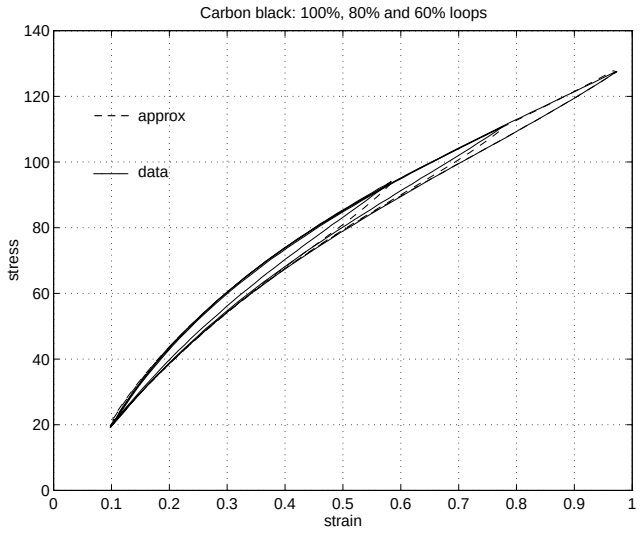

Figure 8: CB rod, response to 100%, 80%, 60% strains: 100% strain parameter set, predicted nested loops for 80%, 60% strains; relative error = 1.1%.

4 Concluding Remarks

In the above presentation we have outlined our progress to date in the development of nonlinear hysteretic dynamic models for MR based elastomers. Substantial experimental validation for our approach is provided in the quasi-static case. Significant efforts are still required to achieve similar status in the full dynamic case. Moreover, to attain the level of modeling required for design and feedback control of active MR elastomers, a major effort remains on response of the elastomer in the presence of an external magnetic field.

5 Acknowledgments

We are grateful to Yue Zhang (current address: Michelin North America) and N.J. Lybeck (current address: Applied Math, Inc.) for their substantial contributions to some of the earlier efforts described above.

We would also like to thank M.J. Gaitens and R. Wilder of Lord Corporation for their help on the actual experiments and on their insightful suggestions on the models.

This research was supported in part by the U.S. Air Force Office of Scientific Research under grants AFOSR F49620-95-1-0236, AFOSR F49620-95-1-0375, and in part by an NSF-GRT fellowship to L.K.P. under grant GER-9454175.

References

[1] H.T. Banks, R.H. Fabiano and Y. Wang, "Estimation of Boltzmann damping coefficients in beam models", *Proceedings of COMCON Workshop on Stabilization of Flexible Structures*, A.V. Balakrishnan and J.P. Zolesio, eds., Optimization Software Inc., New York, (1987) 13-35.

[2] H.T. Banks, R.H. Fabiano and Y. Wang, "Inverse problem techniques for beams with tip body and time hysteresis damping", *Mat. Aplic. e Comput.* **8** (1989) 101-118.

[3] H.T. Banks, R. Fabiano, Y. Wang, D. Inman and H. Cudney, "Spatial versus time hysteresis in damping mechanics", *Proc. 27th IEEE Conf. on Dec. and Control* (1988) 1674-1677.

[4] H.T. Banks, D.S. Gilliam and V.I. Shubov, "Global solvability for damped abstract nonlinear hyperbolic systems", *Differential and Integral Equations* **10** (1997) 309-332.

[5] H.T. Banks and N. Lybeck, "Modeling methodology for elastomer dynamics", *Systems and Control in the 21st Century* (Birkhäuser, Boston, 1996) 37-50.

[6] H.T. Banks, N.J. Lybeck, M.J. Gaitens, B.C. Muñoz and L.C. Yanyo, "Computational methods for estimation in the modeling of nonlinear elastomers", CRSC-TR95-40, NCSU; *Kybernetika* **32** (1996) 526-542.

[7] H.T. Banks, N.G. Medhin, and Y. Zhang, "A mathematical framework for curved active constrained layer structures: well-posedness and approximation", CRSC-TR95-32, NCSU; *Numerical Functional Analysis & Optimization* **17** (1996) 1-22.

[8] H.T. Banks, L.K. Potter and Y. Zhang, "Stress-strain laws for carbon black and silicon filled elastomers", *Proc. 36th IEEE Conf. on Dec. and Control* to appear.

[9] H.T. Banks, R.C. Smith and Y. Wang, *Smart Material Structures: Modeling, Estimation and Control* (Masson, Paris and John Wiley and Sons, Chichester, 1996).

[10] A. Bensoussan, J.L. Lions and G. Papanicolaou, *Asymptotic Analysis for Periodic Structures* (North-Holland, New York, 1978).

[11] H.T. Banks and G.A. Pinter, "Approximation results for parameter estimation in nonlinear elastomers", CRSC-TR96-34, NCSU; *Control and Estimation of Distributed Parameter Systems*, F. Kappel, et.al.,eds., (Birkhäuser, Boston, 1997).

[12] R. Bloch, W.V. Chang and N.W. Tschoegl, "The behavior of rubberlike materials in moderately large deformations", *Journal of Rheology* **22** (1978) 1-32.

[13] R. Bloch, W.V. Chang and N.W. Tschoegl, "On the theory of the viscoelastic behavior of soft polymers in moderately large deformations", *Rheologia Acta* **15** (1976) 367-378.

[14] R.M. Christensen, *Theory of Viscoelasticity: An Introduction*, 2nd ed. (Academic Press, New York, 1982).

[15] M. Codegone and A. Negro, "Homogenization of the nonlinear quasistationary Maxwell equations with degenerated coefficients", *Applicable Analysis* **18** (1984), 159-173.

[16] A. Defranceschi, "An Introduction to Homogenization and G-Convergence", *Lecture Notes, School on Homogenization, ICTP, Trieste, Sept.6-8, 1993.*

[17] M. Doi and M. Edwards, *The Theory of Polymer Dynamics* (Oxford, New York, 1986).

[18] W.N. Findley, J.S. Lai and K. Onaran, *Creep and Relaxation of Nonlinear Viscoelastic Materials*, H.A. Lauwerier and W.T. Koiter, eds., North-Holland Series in Applied Mathematics and Mechanics, (North-Holland Publishing Company, 1976).

[19] J.D. Ferry, *Viscoelastic Properties of Polymers* (John Wiley & Sons, Inc., New York, 1980).

[20] M.I. Friswall, D.J. Inman and M.J. Lam, "On the realisation of GHM models in viscoelasticity", preprint, 1997.

[21] D.F. Golla and P.C. Hughes, "Dynamics of viscoelastic structures — A time-domain, finite element formulation", *ASME J. Applied Mechanics* **52** (1985) 897-905.

[22] V.V. Jikov, S.M. Kozlov and O.A. Oleinik, *Homogenization of Differential Operators and Integral Functionals*, (Springer Verlag, New York, 1994).

[23] A.R. Johnson, C.J. Quigley and J.L. Mead, "Large strain viscoelastic constitutive models for rubber, part I: Formulations", *Rubber Chemistry Technology* **67** (1994) 904-917.

[24] A.R. Johnson, A. Tessler and M. Dambach, "Dynamics of thick elastic beams", *J. Engr. Materials and Tech.* **119** (1997) 278-278.

[25] A.R. Johnson and R.G. Stacer, "Rubber viscoelasticity using the physically constrained systems' stretches as internal variables", *Rubber Chem. Tech.* **66** (1993) 567-577.

[26] M.R. Jolly, J.D. Carlson and B.C. Muñoz, "A model of the behavior of magnetorheological materials", *Smart Mater. Struct.* **5** (1996) 607-614.

[27] M.R. Jolly, J.D. Carlson, B.C. Muñoz and T.A. Bullions, "The magnetoviscoelastic response of elastomer composites consisting of ferrous particles embedded in a polymer matrix", *Journal of Intelligent Material Systems and Structures* **7** (1996) 613-622.

[28] H. Kolsky, "The measurement of the material damping of high polymers over ten decades of frequency and its interpretation", V. K. Kinra and A. Wolfenden, eds., *Mechanics and Mechanisms of Material Damping* (American Society for Testing and Materials, Philadelphia, 1992).

[29] D.J. McTavish, P.C. Hughes, Y. Soucy and W.B. Graham, "Prediction and measurement of modal damping factors for viscoelastic space structures", *AIAA Journal* **30** (1992) 1392-1399.

[30] B.C. Muñoz and M.R. Jolly, "Composites with field responsive rheology", W.K. Brostow, ed., *Performance of Plastics* (Hansen Publisher, N.Y., 1997).

[31] R.W. Ogden, *Non-linear Elastic Deformations* (Ellis Horwood Limited, Chichester, 1984).

[32] F. Reitich and T.M. Simon, "Modeling and computation of the overall magnetic properties of magnetorheological fluids", preprint.

[33] A. Rivera-Dominguez and W.M. Jordan, "Predictive creep response of linear viscoelastic graphite/epoxy composites using the Laplace Transform method", *Journal of Materials Engineering and Performance* **1** (1992) 261-266.

[34] R.A. Schapery, "On the characterization of nonlinear viscoelastic materials", *Polymer Engineering and Science* **9** (1969) 295-310.

[35] Y. Zhang, *Mathematical formulation of vibrations of a composite curved beam structure: Aluminum core material with viscoelastic layers, constraining layers and piezoceramic patches*, Ph.D. Thesis, N.C. State University, May 1997.